Strain effects and band parameters in MgO, ZnO, and CdO

Qimin Yan,[1] Patrick Rinke,[1,2] Momme Winkelnkemper,[3] Abdallah Qteish,[4]
Dieter Bimberg,[3] Matthias Scheffler,[1,2] and Chris G. Van de Walle[1]
[1] *Materials Department, University of California, Santa Barbara, California 93106-5050, USA*
[2] *Fritz-Haber-Institut der Max-Planck-Gesellschaft, Faradayweg 4–6, D-14195 Berlin, Germany*
[3] *Institut für Festkörperphysik, Technische Universität Berlin, Hardenbergstraße 36, D-10623 Berlin, Germany*
[4] *Department of Physics, Yarmouk University, 21163-Irbid, Jordan*
(Dated: September 28, 2012)

We have derived consistent sets of band parameters (bandgaps, crystal-field splittings, effective masses, Luttinger, and E_P parameters) and strain deformation potentials for MgO, ZnO, and CdO in the wurtzite phase. To overcome the limitations of density-functional theory in the local-density and generalized gradient approximations we employ a hybrid functional as well as exact-exchange-based quasiparticle energy calculations in the G_0W_0 approach. We demonstrate that the band and strain parameters derived in this fashion are in very good agreement with the available experimental data and provide predictions for all parameters that have not been determined experimentally so far.

PACS numbers: 71.20.Nr, 71.70.Fk, 78.20.Bh, 85.60.Bt

Renewed interest in the group-II oxides has triggered increased research activity into MgO, ZnO, and CdO and their alloys [1–3]. The group-II oxides are similar to their counterparts, the group-III nitrides, but more earth abundant and are therefore promising candidates for applications as transparent thin-film transistors [4] and optoelectronic devices. ZnO is increasingly being studied on the nanoscale and the growth of a variety of ZnO nanomaterials [5] has been demonstrated. Due to the low growth temperature ZnO-based hybrid organic-inorganic interfaces are now also being explored as optoelectronic and photovoltaic devices [6]. However, unlike the group-III nitrides or III-V semiconductors not all three members of the group-II oxide family have the same equilibrium crystal structure. While ZnO crystalizes in the wurtzite phase, MgO and CdO adopt the rocksalt phase. In spite of this complication wurtzite $Zn_{1-x}Mg_xO$ and $Zn_{1-x}Cd_xO$ alloys with low Mg or Cd concentrations have been grown [7]. The fact that the quantum Hall effect has been observed in a II-VI oxide system [8] demonstrates the quality $ZnO/Zn_{1-x}Mg_xO$ interfaces have reached and confirms that oxide electronics is an emerging field [1, 2].

To aid heterostructure design and nanostructure modeling, essential materials parameters such as band parameters and deformation potentials are required. However, complete and accurate sets of parameters are typically difficult to obtain from experiment alone [9]. For the group-II oxides the situation is further aggravated by the fact that MgO and CdO are not stable in the wurtzite structure. Theoretical results about the electronic properties of wurtzite MgO and CdO are therefore necessary to obtain properties of $Zn_{1-x}Mg_xO$ and $Zn_{1-x}Cd_xO$ alloys by interpolation. We have therefore set out to calculate a complete and consistent set of band parameters and strain deformation potentials for wurtzite MgO, ZnO, and CdO that forms important input for device modeling and for the interpretation of experimental studies.

Due to the lattice mismatch between oxide epilayers and substrates, strain can significantly modify the band structure. The reliable experimental determination of deformation potentials is difficult, and aggravated by the fact that not all strain components can be determined accurately or without further approximations and that the deformation potentials cannot be isolated from each other, because uniaxial and biaxial strain cannot be applied separately. Some experimental results for ZnO have been reported [10, 11], but no experimental data is available for MgO and CdO, which are not stable in the wurtzite phase. Theoretical studies have been performed only for hydrostatic deformation potentials [12]. No comprehensive theoretical study of strain effects in group-II oxide has been conducted up until now. Band (or Luttinger) parameters, on the other hand, have been investigated more extensively [13–15]. However, all but one study [15] was affected by the bandgap problem associated with density-functional theory based on the local-density approximation (LDA) or generalized gradient approximation [9, 16].

In this work, we present a complete set of band dispersion parameters (effective masses and Luttinger parameters) and deformation potentials ($a_{cz} - D_1$, $a_{ct} - D_2$, D_3, D_4, D_5, and D_6) for the group-II oxides MgO, ZnO, and CdO in the wurtzite phase. The structural relaxations with strain perturbations are performed using the plane-wave projector augmented wave method (PAW) as implemented in the VASP code [17]. We use the Heyd-Scuseria-Ernzerhof hybrid exchange-correlation functional [18] with a screening parameter μ=0.2 and a mixing parameter of α=0.25 (HSE06). In previous work we showed that HSE06 gives accurate lattice parameters and bandgaps in good agreement with experiment for the group-III nitrides [19]. We use a 6×6×4 Γ-point centered k-point mesh and a plane-wave cutoff of 600 eV; such a high level of convergence is essential in order to accurately determine the internal displacement parameter u. To determine the band parameters we fit a $\mathbf{k}\cdot\mathbf{p}$ Hamiltonian to high-resolution band structures around the Γ-point as described in Ref. 9. The band structures at the Γ-point have been computed in both HSE06 and the G_0W_0@OEPx(cLDA) approach [20] (the latter stands for quasiparticle energy calculations based on optimized-effective-potential exact-exchange ground

TABLE I. Equilibrium lattice parameters (a, c, and u) obtained with HSE06 and bandgaps (E_g) and crystal-field splitting Δ_{cr} obtained with both HSE06 and the G_0W_0@OEPx(cLDA) method at HSE06 equilibrium lattice parameters. For ZnO, experimental lattice parameters at $T = 300$ K, bandgap at $T = 300$ K and crystal-field splitting values are included for comparison (from Refs. 26 and 27).

	method	a (Å)	c (Å)	u	E_g (eV)	Δ_{cr} (meV)
MgO	HSE06	3.278	5.062	0.3919	5.21	-346
	G_0W_0	-	-	-	7.16	-402
ZnO	HSE06	3.264	5.238	0.3807	2.48	66
	G_0W_0	-	-	-	3.26	74
	Exp.	3.249	5.205	-	3.43	43
CdO	HSE06	3.652	5.739	0.3878	1.13	117
	G_0W_0	-	-	-	1.23	145

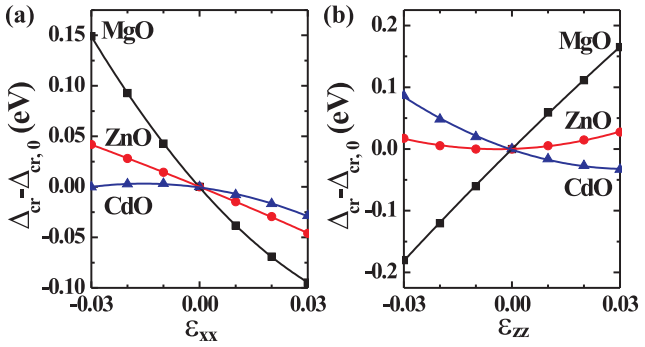

FIG. 1. The change in crystal-field splitting (Δ_{cr}) from its unstrained value ($\Delta_{cr,0}$) for wurzite MgO, ZnO, and CdO under (a) biaxial strain in the c plane and (b) uniaxial strain along the c axis.

states that include LDA correlation) using the *GW* space-time code `gwst` [21] linked to the plane-wave, pseudopotential density-functional theory code `S/PHI/nX` [22]. Consistent norm-conserving OEPx(cLDA) pseudopotentials as described in Ref. 20 are used for the *GW* and OEPx(cLDA) calculations. We have carefully checked the convergence of the G_0W_0 calculations, in light of concerns raised by Shih *et al.* [23] and Friedrich *et al.* [24], verifying that our G_0W_0@OEPx(cLDA) calculations, which yield a ZnO gap of 3.26 eV, are converged both with respect to plane-wave cutoff and number of unoccupied states [25].

Equilibrium lattice parameters obtained with HSE06 (Table I) agree very well with experiment for ZnO (¡1% overestimation). Bandgaps and crystal-field splitting (Δ_{cr}) obtained from both G_0W_0@OEPx(cLDA) and HSE06 calculations at HSE06 equilibrium lattice parameters are listed in Table I. Note that while the HSE06 functional greatly improves the bandgap of ZnO (2.48 eV) compared to PBE calculations (1.18 eV), it still underestimates the fundamental bandgap. The bandgap for ZnO with G_0W_0@OEPx(cLDA) calculations agrees very well with experiment (to within 0.2 eV). The crystal-field splitting is positive for CdO and ZnO, while for MgO it is negative.

Four types of strain components may be present in the wurtzite system: isotropic biaxial strain in the c plane ($\varepsilon_\perp = \varepsilon_{xx} + \varepsilon_{yy}$, with $\varepsilon_{xx} = \varepsilon_{yy}$), anisotropic biaxial strain in the c plane ($|\varepsilon_{xx} - \varepsilon_{yy}|$, with $\varepsilon_{xx} \neq \varepsilon_{yy}$), uniaxial strain along the c axis (ε_{zz}), and shear strain (ε_{xz} and ε_{yz}). Using the $\mathbf{k}\cdot\mathbf{p}$ method, strain components are treated as perturbations in the Hamiltonian and the modifications of the band structure by strain are quantified by conduction-band deformation potentials (a_{cz} and a_{ct}) and valence-band deformation potentials (D_1 to D_6). By applying strain and fitting the eigenenergies of the 6×6 $\mathbf{k}\cdot\mathbf{p}$ Hamiltonian [28] to first-principles band structures at the Γ-point, we can obtain all deformation potentials [19, 29]. In this work we determined all deformation potentials from HSE06 calculations. Explicitly performing G_0W_0@OEPx(cLDA) calculations for all strain configurations would be prohibitive; for nitrides, we verified that deformation potentials obtained from G_0W_0@OEPx(cLDA) calculations and from HSE06 agree to within 0.40 eV [19].

TABLE II. Deformation potentials (in eV) of wurtzite MgO, ZnO, and CdO obtained by HSE06 calculations. Experimental data for ZnO are also shown.

	Method	$a_{cz} - D_1$	$a_{ct} - D_2$	D_3	D_4	D_5	D_6
MgO	HSE06	-1.95	-7.96	5.87	-1.97	-1.93	-3.03
ZnO	HSE06	-3.06	-2.46	0.47	-0.84	-1.21	-1.77
	Exp. [a]	-3.80	-3.80	0.80	-1.40	-1.20	-2.0 [b]
	Exp. [c]	-3.90	-4.13	1.15	-1.22	-1.53	-2.88 [b]
CdO	HSE06	-2.81	-0.29	-1.86	-0.30	-0.91	-1.21

[a] Reference 10.
[b] Only the magnitude of D_6 was obtained in this experiment.
[c] Reference 11.

As shown in Figure 1, the change of the crystal-field splitting (Δ_{cr}) in wurtzite MgO, ZnO, and CdO under biaxial strain in the c plane and uniaxial strain along the c axis (ε_{zz}) is nonlinear. This implies that the deformation potentials vary with lattice parameters, as previously observed for group-III nitrides [19]; the behavior can be well described with a parabolic fit. We focus on the linear regime in the vicinity of the experimental lattice parameters for ZnO, and around the HSE06 equilibrium lattice parameters for MgO and CdO (where no experimental data are available).

A complete set of deformation potentials from HSE06 calculations is listed in Table II. With the exception of $a_{cz} - D_1$ the deformation potentials increase as the bandgap increases from CdO to ZnO and MgO, showing the same trend as in the group-III nitrides (deformation potentials increase from InN to GaN and AlN) [19]. Differing from ZnO and MgO, the deformation potential D_3 of CdO is negative, which is consistent with the change of Δ_{cr} under uniaxial strain as shown in Figure 1(b). Compared with GaN, the deformation potentials of ZnO are much smaller in magnitude. The experimental data[10, 11] for ZnO are included for comparison. Generally HSE06 results show good agreement with experimental data.

Our first-principles calculations also indicate that the

TABLE III. Luttinger parameters (A_7 is in eV Å, all others are dimensionless) and transition matrix elements E_P (in eV) of wurtzite MgO, ZnO, and CdO obtained with both HSE06 and the G_0W_0@OEPx(cLDA) approaches. The effective masses are derived from the Luttinger parameters using the "near- Γ" approximation [9] and the spin-orbit splittings reported by Schleife *et al.* [15]

param.	MgO		ZnO		CdO	
method	HSE06	G_0W_0	HSE06	G_0W_0	HSE06	G_0W_0
A_1	−2.888	−2.709	−2.747	−2.743	−3.298	−3.154
A_2	−0.199	−0.211	−0.386	−0.393	−0.380	−0.393
A_3	2.732	2.546	2.386	2.377	2.936	2.770
A_4	−0.495	−0.484	−2.089	−2.069	−3.783	−3.810
A_5	−0.687	−0.692	−2.059	−2.051	−3.685	−3.711
A_6	−1.411	−1.295	−2.103	−2.099	−3.643	−2.786
A_7	−0.133	−0.119	0.028	0.001	−0.046	−0.010
$E_P^{\parallel}$	3.932	3.801	12.443	13.042	9.341	10.638
$E_P^{\perp}$	6.835	6.899	9.658	9.604	6.258	7.224
$m_e^{\parallel}$	0.369	0.379	0.239	0.246	0.168	0.173
$m_e^{\perp}$	0.371	0.383	0.244	0.250	0.154	0.150
$m_{\Gamma 9}^{\parallel}$	6.416	6.105	2.769	2.732	2.755	2.603
$m_{\Gamma 9}^{\perp}$	1.441	1.441	0.404	0.406	0.240	0.238
$m_{\Gamma 7+v}^{\parallel}$	0.347	0.370	2.563	2.567	2.442	2.416
$m_{\Gamma 7+v}^{\perp}$	4.982	4.727	0.408	0.410	0.244	0.240
$m_{\Gamma 7-v}^{\parallel}$	6.132	5.923	0.368	0.368	0.306	0.320
$m_{\Gamma 7-v}^{\perp}$	1.444	1.443	2.434	2.417	2.271	2.304

quasicubic approximation [19] breaks down for the group-II wurtzite oxide system. In the quasicubic approximation, the deformation potentials are related as follows: $D_3 + 2D_4 = 0$, $D_1 + D_3 = D_2$ and $D_3 + 4D_5 = \sqrt{2}D_6$. However, we find that $D_3 + 2D_4$ is equal to 1.93 eV for MgO, -1.21 eV for ZnO, and -2.46 eV for CdO, i.e., significantly different from zero. Due to the lack of experimental data for wurtzite MgO and CdO, the deformation potentials of ZnO have been used over the entire alloy range in device modeling of group-II oxide alloys [30]. Our calculations show that this is a poor approximation: the variation of deformation potentials among the three oxides is large, and independent sets of deformation potentials for MgO and CdO are necessary for accurate device simulations.

The calculated effective masses, Luttinger parameters, and transition matrix element E_P of wurtzite MgO, ZnO, and CdO with both the HSE06 and the G_0W_0@OEPx(cLDA) approach are shown in Table III. Generally the effective masses and Luttinger parameters obtained by HSE06 agree very well with the G_0W_0@OEPx(cLDA) ones. This implies that HSE06 produces conduction- and valence-band dispersions that are very similar to those of G_0W_0. Our effective masses are in overall good agreement with recent quasiparticle calculations [15, 31, 32].

It is remarkable that, in contrast to the group-III nitrides [9], the Luttinger parameters in the group-II oxides are fairly similar across the oxide series. For example, the A_1 parameter in the nitrides varies from -3.991 in AlN to -15.803 in InN (a difference of a factor of 3.96) and A_6 from -1.952 to -10.078 (a difference of a factor of 5.16), whereas in the oxides the corresponding variations are only by factors of 1.16 and 2.15. For A_4 and A_5 the variations across the respective series are more similar, although the absolute magnitudes of the parameters are larger in the nitrides (A_4: -1.147 (AlN) to -7.151 (InN) and A_5: -1.329 (AlN) to -7.060 (InN)). Another noteworthy observation is the fact that, unlike in the nitrides, the E_P parameters in the oxides are highly anisotropic.

Since the bandgap calculated from HSE06 for the oxides is in worse agreement with G_0W_0 and experiment than it is for the nitrides, we check whether the band parameters and deformation potentials can be improved by modifying the mixing parameter. For ZnO, as a test case, we modify the mixing parameter (α=0.36) to reproduce the experimental bandgap (3.41 eV) and calculate the band parameters and deformation potentials of ZnO [32]. Note that the changes in deformation potentials are less than 0.3 eV, and the changes in band parameters are also very small. This check indicates that the choice of the mixing parameter for ZnO only slightly affects the calculated parameters, which is reassuring. We hence believe that the deformation potentials and band parameters listed in the tables with default HSE06 parameters are reliable.

Note that the linear interpolation between binary compounds when describing alloy properties is only an approximation and there may be some nonlinearities in different physical quantities of ZnXO (X = Cd, Mg) alloys. For example, the nonlinearity in the bandgap has been quantified as a bowing parameter and this parameter has been measured experimentally. Special attention regarding such nonlinearities should be paid when using these band parameters and deformation potentials to describe electronic properties of ZnXO alloys.

In conclusion, we have presented a systematic study of the band dispersion and strain effects on electronic band structures of the group-II-oxides MgO, ZnO and CdO. Using hybrid functional calculations, we report a consistent and complete set of deformation potentials that describes band-structure modifications in the presence of strain. We also obtain a consistent set of band parameters that agrees well with values obtained with G_0W_0@OEPx(cLDA). These first-principles deformation potentials and band parameters provide a solid foundation for an accurate modeling of oxide-based device structures.

This work was supported by the Solid State Lighting and Energy Center at the University of California, Santa Barbara. P.R. acknowledges the support of the Deutsche Forschungsgemeinschaft, the UCSB-MPG Program for International Exchange in Materials Science, and the NSF-IMI Program (DMR08-43934). We acknowledge the use of the CSC/CNSI/MRL Computing resources (NSF-CNS-09-60316 and DMR11-21053) as well as TeraGrid (NSF DMR07-0072N).

[1] A. P. Ramirez, Science **315**, 1377 (2007).

[2] A. Janotti and C. G. Van de Walle, Rep. Prog. Phys. **72**, 126501 (2009).

[3] H. von Wenckstern, R. Schmidt-Grund, C. Bundesmann, A. Müller, C.P. Dietrich, M. Stölzel, M. Lange, M. Grundmann *The (Mg,Zn)O Alloy Handbook of Zinc Oxide and Related Materials, Vol. 1 Materials* (Taylor and Francis/CRC Press, Florida, USA) 2011.

[4] H. Frenzel, A. Lajn, H. von Wenckstern, M. Lorenz, F. Schein, Z. Zhang, and M. Grundmann, Adv. Mater. **22**, 5332 (2010).

[5] X. Wang, C. J. Summers, and Z. L. Wang, Nano Lett. **4**, 423 (2004).

[6] S. Blumstengel, S. Sadofev, C. Xu, J. Puls, R. L. Johnson, H. Glowatzki, N. Koch, and F. Henneberger, Phys. Rev. B **77**, 085323 (2008).

[7] S. Sadofev, S. Blumstengel, J. Cui, J. Puls, S. Rogaschewski, P. Schäfer, Y. G. Sadofyev, and F. Henneberger, Appl. Phys. Lett. **87**, 098903 (2005).

[8] A. Tsukazaki, A. Ohtomo, T. Kita, Y. Ohno, H. Ohno, and M. Kawasaki, Science **315**, 1388 (2007).

[9] P. Rinke, M. Winkelnkemper, A. Qteish, D. Bimberg, J. Neugebauer, and M. Scheffler, Phys. Rev. B **77**, 075202 (2008).

[10] D. W. Langer and R. N. Euwema, Phys. Rev. B **2**, 4005 (1970).

[11] J. Wrzesinski and D. Frohlich, Phys. Rev. B **56**, 13087 (1997).

[12] A. Janotti and C. G. Van de Walle, Phys. Rev. B **75**, 121201 (2007).

[13] W. J. Fan, J. B. Xia, P. A. Agus, S. T. Tan, S. F. Yu, and X. W. Sun, J. Appl. Phys. **99**, 013702 (2006).

[14] H. Rozale, B. Bouhafs, and P. Ruterana, Superlattice Microst. **42**, 165 (2007).

[15] A. Schleife, F. Fuchs, C. Rödl, J. Furthmüller, and F. Bechstedt, Phys. Status Solidi B **246**, 2150 (2009).

[16] Q. Yan, P. Rinke, M. Scheffler, and C. G. Van de Walle, Semicond. Sci. Technol. **26**, 014037 (2011).

[17] G. Kresse and J. Furthmüller, Phys. Rev. B **54**, 11169 (1996).

[18] J. Heyd, G. E. Scuseria, and M. Ernzerhof, J. Chem. Phys. **124**, 219906 (2006).

[19] Q. Yan, P. Rinke, M. Scheffler, and C. G. Van de Walle, Appl. Phys. Lett. **95**, 121111 (2009).

[20] P. Rinke, A. Qteish, J. Neugebauer, C. Freysoldt, and M. Scheffler, New J. Phys. **7**, 126 (2005).

[21] M. M. Rieger, L. Steinbeck, I. White, H. Rojas, and R. Godby, Comput. Phys. Commun. **117**, 211 (1999).

[22] S. Boeck, C. Freysoldt, A. Dick, L. Ismer, and J. Neugebauer, Comput. Phys. Commun. **182**, 543 (2011).

[23] B.-C. Shih, Y. Xue, P. Zhang, M. L. Cohen, and S. G. Louie, Phys. Rev. Lett. **105**, 146401 (2010).

[24] C. Friedrich, M. C. Müller, and S. Blügel, Phys. Rev. B **83**, 081101(R) (2011).

[25] See supplementary material at [URL will be inserted by AIP] for details of convergence studies.

[26] O. Madelung, ed., *Semiconductors-Basic Data, 2nd revised ed.* (Springer, Berlin, 1996).

[27] D. C. Reynolds, D. C. Look, B. Jogai, C. W. Litton, G. Cantwell, and W. C. Harsch, Phys. Rev. B **60**, 2340 (1999).

[28] G. L. Bir and G. E. Pikus, *Symmetry and Strain-Induced Effects in Semiconductors* (Wiley, New York, 1974).

[29] Q. Yan, P. Rinke, M. Scheffler, and C. G. Van de Walle, Appl. Phys. Lett. **97**, 181102 (2010).

[30] W. Fan, A. Abiyasa, S. Tan, S. Yu, X. Sun, J. Xia, Y. Yeo, M. Li, and T. Chong, J. Cryst. Growth **287**, 28 (2006).

[31] See supplementary material at [URL will be inserted by AIP] for details of effective mass calculations and comparison.

[32] See supplementary material at [URL will be inserted by AIP] for the dependence of band parameters and deformation potentials of ZnO on the mixing parameter.